The Kontsevich tetrahedral flow revisited

Bouisaghouane, A.; Buring, R.; Kiselev, A.

Published in:
Journal of geometry and physics

DOI:
10.1016/j.geomphys.2017.04.014

Publication date:
2017

Journal of Geometry and Physics 119 (2017) 272–285

Contents lists available at ScienceDirect

Journal of Geometry and Physics

journal homepage: www.elsevier.com/locate/geomphys

The Kontsevich tetrahedral flow revisited

A. Bouisaghouane *, R. Buring, A. Kiselev [1,2]

Johann Bernoulli Institute for Mathematics and Computer Science, University of Groningen, The Netherlands

ARTICLE INFO

Article history:
Received 24 November 2016
Received in revised form 13 March 2017
Accepted 30 April 2017
Available online 12 May 2017

MSC:
53D55
58E30
81S10
secondary 53D17
58Z05
70S20

Keywords:
Poisson bracket
Affine manifold
Graph complex
Tetrahedral flow
Poisson cohomology

ABSTRACT

We prove that the Kontsevich tetrahedral flow $\dot{\mathcal{P}} = \mathcal{Q}_{a:b}(\mathcal{P})$, the right-hand side of which is a linear combination of two differential monomials of degree four in a bi-vector $\mathcal{P}$ on an affine real Poisson manifold N^n, does infinitesimally preserve the space of Poisson bi-vectors on N^n if and only if the two monomials in $\mathcal{Q}_{a:b}(\mathcal{P})$ are balanced by the ratio $a : b = 1 : 6$. The proof is explicit; it is written in the language of Kontsevich graphs.

0. Introduction

The main question which we address in this paper is how Poisson structures can be deformed in such a way that they stay Poisson. We reveal one such method that works for all Poisson structures on affine real manifolds; the construction of that flow on the space of bi-vectors was proposed in [1]: the formula is derived from two differently oriented tetrahedral graphs on four vertices. The flow is a linear combination of two terms, each quartic-nonlinear in the Poisson structure. By using several examples of Poisson brackets with high polynomial degree coefficients, the first and last authors demonstrated in [2] that the ratio 1 : 6 is the only possible balance at which the tetrahedral flow can preserve the property of the Cauchy datum to be Poisson. But does the Kontsevich tetrahedral flow $\dot{\mathcal{P}} = \mathcal{Q}_{1:6}(\mathcal{P})$ with ratio 1 : 6 actually preserve the space of *all* Poisson bi-vectors?

We prove the infinitesimal version of this claim: namely, we show that $[\![\mathcal{P}, \mathcal{Q}_{1:6}(\mathcal{P})]\!] = 0$ for every bi-vector $\mathcal{P}$ satisfying the master-equation $[\![\mathcal{P}, \mathcal{P}]\!] = 0$ for Poisson structures. The proof is graphical: to prove that Eq. (2) holds, we find an operator $\Diamond$, encoded by using the Kontsevich graphs, that solves equation (10). We also show that there is no universal mechanism (that would involve the language of Kontsevich graphs) for the tetrahedral flow to be trivial in the respective Poisson cohomology.

* Correspondence to: Johann Bernoulli Institute for Mathematics and Computer Science, University of Groningen, P.O. Box 407, 9700 AK Groningen, The Netherlands.
E-mail address: A.V.Kiselev@rug.nl (A. Kiselev).
1 Institut des Hautes Études Scientifiques, 35 route de Chartres, Bures-sur-Yvette, F-91440 France.
2 Present address: Max Planck Institute for Mathematics, Vivatsgasse 7, D-53111 Bonn, Germany.

http://dx.doi.org/10.1016/j.geomphys.2017.04.014
0393-0440/

The text is structured as follows. In Section 1 we recall how oriented graphs can be used to encode differential operators acting on the space of multivectors. In particular, differential polynomials in a given Poisson structure are obtained as soon as a copy of that Poisson bi-vector is placed in every internal vertex of a graph. Specifically, the right-hand side $\mathcal{Q}_{a:b} = a \cdot \Gamma_1 + b \cdot \Gamma_2$ of the Kontsevich tetrahedral flow $\dot{\mathcal{P}} = \mathcal{Q}_{a:b}(\mathcal{P})$ on the space of bi-vectors on an affine Poisson manifold $\big(N^n, \mathcal{P}\big)$ is a linear combination of two differential monomials, $\Gamma_1(\mathcal{P})$ and $\Gamma_2(\mathcal{P})$, of degree four in the bi-vector $\mathcal{P}$ that evolves.

We determine at which balance $a : b$ the Kontsevich tetrahedral flow $\dot{\mathcal{P}} = \mathcal{Q}_{a:b}(\mathcal{P})$ infinitesimally preserves the space of Poisson bi-vectors, that is, the bi-vector $\mathcal{P} + \varepsilon\mathcal{Q}_{a:b}(\mathcal{P}) + \bar{o}(\varepsilon)$ satisfies the equation

$$[\![\mathcal{P} + \varepsilon\mathcal{Q}_{a:b}(\mathcal{P}) + \bar{o}(\varepsilon), \mathcal{P} + \varepsilon\mathcal{Q}_{a:b}(\mathcal{P}) + \bar{o}(\varepsilon)]\!] \doteq \bar{o}(\varepsilon) \qquad \text{via } [\![\mathcal{P}, \mathcal{P}]\!] = 0; \tag{1}$$

here we denote by $[\![\cdot, \cdot]\!]$ the Schouten bracket (see formula (5)). Expanding, we obtain the cocycle condition,

$$[\![\mathcal{P}, \mathcal{Q}_{a:b}(\mathcal{P})]\!] \doteq 0 \qquad \text{via } [\![\mathcal{P}, \mathcal{P}]\!] = 0, \tag{2}$$

with respect to the Poisson differential $\boldsymbol{\partial}_{\mathcal{P}} = [\![\mathcal{P}, \cdot]\!]$. Viewed as an equation with respect to the ratio $a : b$, condition (2) is the main object of our study.

Recent counterexamples [2] show that the bi-vector $\mathcal{P} + \varepsilon\mathcal{Q}_{a:b}(\mathcal{P}) + \bar{o}(\varepsilon)$ can stay Poisson *only if* the balance $a : b$ in $\mathcal{Q}_{a:b}$ is equal to $1 : 6$. We now prove the infinitesimal part of sufficiency: the deformation $\mathcal{P} + \varepsilon\mathcal{Q}_{1:6}(\mathcal{P}) + \bar{o}(\varepsilon)$ is always infinitesimally Poisson, whence the balance $a : b = 1 : 6$ in the Kontsevich tetrahedral flow is universal for all Poisson bi-vectors $\mathcal{P}$ on all affine manifolds N^n. The proof is explicit: in Section 2 we reveal the mechanism of factorization – via the Jacobi identity – in (2) at $a : b = 1 : 6$. On the left-hand side of factorization problem (2) we expand the Poisson differential of the Kontsevich tetrahedral flow at the balance $1 : 6$ into the sum of 39 graphs (see Fig. 3 and Table 2 in Appendix A). On the other side of that factorization, we take the sum that runs with undetermined coefficients over all those fragments of differential consequences of the Jacobi identity $[\![\mathcal{P}, \mathcal{P}]\!] = 0$ which are known to vanish independently. We then find a linear polydifferential operator $\Diamond(\mathcal{P}, \cdot)$ that acts on the filtered components of the Jacobiator $\mathrm{Jac}(\mathcal{P}) := [\![\mathcal{P}, \mathcal{P}]\!]$ for the bi-vector $\mathcal{P}$; the operator $\Diamond$ provides the factorization $[\![\mathcal{P}, \mathcal{Q}_{1:6}(\mathcal{P})]\!](f, g, h) = \Diamond\big(\mathcal{P}, \mathrm{Jac}(\mathcal{P})(\cdot, \cdot, \cdot)\big)(f, g, h)$ of the $\boldsymbol{\partial}_{\mathcal{P}}$-cocycle condition, see (2), through the Jacobi identity $\mathrm{Jac}(\mathcal{P}) = 0$. To describe the differential operators that produce such consequences of the Jacobi identity, we use the pictorial language of graphs: every internal vertex contains a copy of the bi-vector $\mathcal{P}$ and the operators are reduced by using its skew-symmetry. There remain 7,025 graphs, the coefficients of which are linear in the unknowns. We now solve the arising inhomogeneous linear algebraic system. Its solution yields a polydifferential operator $\Diamond$, encoded using Leibniz graphs, that provides the sought-for factorization $[\![\mathcal{P}, \mathcal{Q}_{1:6}]\!] = \Diamond(\mathcal{P}, \mathrm{Jac}(\mathcal{P}))$. It is readily seen from formula (11) that this operator $\Diamond$ is completely determined by only 8 nonzero coefficients (out of 1132 total).[3] Therefore, although finding an operator $\Diamond$ was hard, verifying that it does solve the factorization problem has become almost immediate, as we show in the proof of Theorem 3. We thereby establish the main result (namely, Corollary 4). The paper concludes with the formulation of an open problem about the integration of tetrahedral flow in (1) to higher order expansions in ε, see (13).

In Appendix B we outline a different method to tackle the factorization problem, namely, by making the Jacobi identity visible in (2) by perturbing the original structure $\mathcal{P} \mapsto \widetilde{\mathcal{P}}$ in such a way that $\widetilde{\mathcal{P}}$ is not Poisson and $\mathcal{Q}_{1:6}(\widetilde{\mathcal{P}}) \neq 0$. Hence $\widetilde{\mathcal{P}}$ contributes to the right-hand side of (2) such that the respectively perturbed bi-vector $\mathcal{Q}_{1:6}(\widetilde{\mathcal{P}})$ stops being compatible with the perturbed Poisson structure $\widetilde{\mathcal{P}}$. The first-order balance of both sides of perturbed equation (2) then suggests the coefficients of those differential consequences of the Jacobiator which are actually involved in the factorization mechanism. The coefficients of operators realized by graphs which were found by following this scheme are reproduced in the full run-through that gave us the solution $\Diamond$ in Section 2.

1. The main problem: From graphs to multivectors

1.1. The language of graphs

Let us formalize a way to encode polydifferential operators – in particular multivectors – using oriented graphs [3,4]. In an affine real manifold N^n (here $2 \leqslant n < \infty$), take a chart $U_\alpha \hookrightarrow \mathbb{R}^n$ and denote the Cartesian coordinates by $\boldsymbol{x} = (x^1, \ldots, x^n)$. We now consider only the oriented graphs whose vertices are either tails for an ordered pair of arrows, each decorated with its own index, or sinks (with no issued edges) like the vertices *1, 2* in $(1) \overset{i}{\leftarrow} \bullet \overset{j}{\rightarrow} (2)$. The arrowtail vertices are called *internal*. Every internal vertex $\bullet$ carries a copy of a given Poisson bi-vector $\mathcal{P} = \mathcal{P}^{ij}(\boldsymbol{x})\,\partial_i \wedge \partial_j$ with its own pair of indices. For each internal vertex $\bullet$, the pair of out-going edges is ordered $\mathrm{L} \prec \mathrm{R}$. The ordering $\mathrm{L} \prec \mathrm{R}$ of decorated out-going edges coincides with the ordering "first $\prec$ second" of the indices in the coefficients of $\mathcal{P}$. Namely, the left edge (L) carries the first index and the other edge (R) carries the second index. By definition, the decorated edge $\bullet \overset{i}{\rightarrow} \bullet$ denotes at once the derivation $\partial/\partial x^i \equiv \partial_i$ (that acts on the content of the arrowhead vertex) and the summation $\sum_{i=1}^{n}$ (over the index i in the object which is contained within the arrowtail vertex). As it has been explained in [5,6], the operator which every graph encodes is equal to the sum (running over all the indices) of products (running over all the vertices) of those vertices content (differentiated by the in-coming arrows, if any). Moreover, we let the sinks be ordered (like $1 \prec 2$ above), so that every such graph defines a polydifferential operator: its arguments are thrown into the respective sinks.

[3] The maximally detailed description of that solution $\Diamond$ is contained in Appendix A.

Fig. 1. A tadpole and an "eye".

Example 1. The *wedge graph* $(1) \overset{i}{\underset{L}{\leftarrow}} \mathcal{P}^{ij}(\boldsymbol{x}) \overset{j}{\underset{R}{\rightarrow}} (2)$ encodes the bi-differential operator $\sum_{i,j=1}^{n}(1)\overleftarrow{\partial_i}\cdot\mathcal{P}^{ij}(\boldsymbol{x})\cdot\overrightarrow{\partial_j}(2)$. Such graph specifies a Poisson bracket (on every chart $U_\alpha \subseteq N^n$) if it satisfies the Jacobi identity, see (4).

Remark 1. In principle, we allow the presence of both the tadpoles and cycles over two vertices (or "eyes"), see Fig. 1. However, in hindsight there will be neither tadpoles nor eyes in the solution which we shall have found in Section 2.

Remark 2. Under the above assumptions, there exist inhabited graphs that encode zero differential operators. Namely, consider the graph with a double edge:

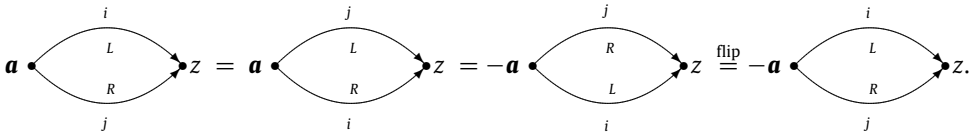

By first relabelling the summation indices and then swapping $\mathrm{L} \rightleftarrows \mathrm{R}$ (and redrawing) we evaluate the operator acting at z to $\sum_{i,j=1}^{n} a^{ij}\partial_i\partial_j(z) = -\sum_{i,j=1}^{n} a^{ij}\partial_i\partial_j(z)$; whence the operator is zero. In the same way, any graph containing a double edge encodes a zero operator. Graphs can also encode zero differential operators in a more subtle way. For example consider the wedge on two wedges:

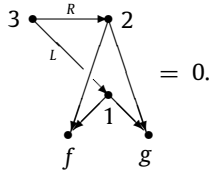

$$= 0. \tag{3}$$

Swapping the labels $1 \rightleftarrows 2$ of the lower wedges does not change the operator. On the other hand, doing the same in a different way, namely, by swapping 'left' and 'right' in the top wedge introduces a minus sign. Hence the graph encodes a differential operator equal to minus itself, i.e. zero. Proving that a graph which contains the left-hand side of (3) as a subgraph equals zero is an elementary exercise (cf. Example 3).

Besides the trivial vanishing mechanism in Remark 2, there is the Jacobi identity together with its differential consequences, which will play a key role in what follows. For any three arguments $1, 2, 3 \in C^\infty(N^n)$, the Jacobi identity $\mathrm{Jac}_{\mathcal{P}}(1, 2, 3) = 0$ is realized[4] by the graph

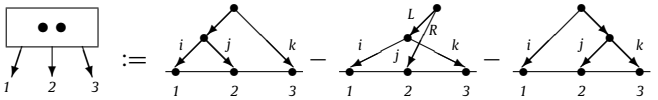

(4)

In our notation this identity's left-hand side encodes a sum over all (i, j, k); instead restricting to fixed (i, j, k) corresponds to taking a coefficient of the differential operator (cf. Lemma 1), which yields the respective component $\mathrm{Jac}_{\mathcal{P}}^{ijk}$ of the Jacobiator $\mathrm{Jac}(\mathcal{P})$. Clearly, the Jacobiator is totally skew-symmetric with respect to its arguments *1, 2, 3* .

In fact, the Jacobiator $\mathrm{Jac}(\mathcal{P})$ is the *Schouten bracket* of a given Poisson bi-vector $\mathcal{P}$ with itself: $\mathrm{Jac}(\mathcal{P}) = [\![\mathcal{P}, \mathcal{P}]\!]$ (depending on conventions, times a constant which is here omitted, cf. [7]). The bracket $[\![\cdot, \cdot]\!]$ is a unique extension of the commutator $[\cdot, \cdot]$ on the space of vector fields $\mathfrak{X}^1(N^n)$ to the space $\mathfrak{X}^*(N^n)$ of multivector fields. Let us recall its inductive definition in the finite-dimensional set-up.

Definition 1. The Schouten bracket $[\![\cdot, \cdot]\!] : \mathfrak{X}^*(N^n) \times \mathfrak{X}^*(N^n) \to \mathfrak{X}^*(N^n)$ coincides with the commutator $[\cdot, \cdot]$ when evaluated on 1-vectors; when evaluated at a p-vector $\mathfrak{X}$, q-vector $\mathfrak{Y}$, and r-vector $\mathfrak{Z}$ for $p, q, r \geqslant 1$, the Schouten bracket is shifted-graded skew-symmetric, $[\![\mathfrak{X}, \mathfrak{Y}]\!] = -(-1)^{(p-1)(q-1)}[\![\mathfrak{Y}, \mathfrak{X}]\!]$, and it works over each argument via the graded Leibniz rule: $[\![\mathfrak{X}, \mathfrak{Y} \wedge \mathfrak{Z}]\!] = [\![\mathfrak{X}, \mathfrak{Y}]\!] \wedge \mathfrak{Z} + (-1)^{(p-1)q}\mathfrak{Y} \wedge [\![\mathfrak{X}, \mathfrak{Z}]\!]$. The bracket is then extended by linearity from homogeneous components to the entire space of multivector fields on N^n.

[4] The notation $\mathrm{Jac}_{\mathcal{P}}(1, 2, 3)$ is synonymic to $\mathrm{Jac}(\mathcal{P})(1 \otimes 2 \otimes 3)$.

Remark 3. The construction of Schouten bracket also reads as follows. Denote by ξ_i the parity-odd canonical conjugate of the variable x^i for every $i = 1, \ldots, n$. For instance, every bi-vector is realized in terms of local coordinates x^i and ξ_i on ΠT^*N^n by using $\mathcal{P} = \frac{1}{2}\langle \xi_i \mathcal{P}^{ij}(\boldsymbol{x})\xi_j\rangle$. The Schouten bracket $[\![\cdot,\cdot]\!]$ is the parity-odd Poisson bracket which is locally determined on ΠT^*N^n by the canonical symplectic structure $\mathrm{d}\boldsymbol{x}\wedge\mathrm{d}\boldsymbol{\xi}$. Our working formula is[5]

$$[\![\mathcal{P},\mathcal{Q}]\!] = (\mathcal{P})\frac{\overleftarrow{\partial}}{\partial x^i}\cdot\frac{\overrightarrow{\partial}}{\partial \xi_i}(\mathcal{Q}) - (\mathcal{P})\frac{\overleftarrow{\partial}}{\partial \xi_i}\cdot\frac{\overrightarrow{\partial}}{\partial x^i}(\mathcal{Q}). \tag{5}$$

It is now readily seen that the Schouten bracket of homogeneous arguments satisfies its own, shifted-graded Jacobi identity,

$$[\![\mathcal{X},[\![\mathcal{Y},\ \cdot\ ]\!]]\!](\mathcal{Z}) - (-)^{(|\mathcal{X}|-1)\cdot(|\mathcal{Y}|-1)}[\![\mathcal{Y},[\![\mathcal{X},\ \cdot\ ]\!]]\!](\mathcal{Z}) = [\![[\![\mathcal{X},\mathcal{Y}]\!],\ \cdot\ ]\!](\mathcal{Z}).$$

Hence for a bi-vector $\mathcal{P}$ such that $[\![\mathcal{P},\mathcal{P}]\!] = 0$, the map $\boldsymbol{\partial}_{\mathcal{P}} = [\![\mathcal{P},\cdot]\!] : \mathfrak{X}^{\ell}(N^n) \to \mathfrak{X}^{\ell+1}(N^n)$ is a differential.

Remark 4. The graphical calculation of the Schouten bracket $[\![\cdot,\cdot]\!]$ of two arguments amounts to the action – via the Leibniz rule – of every out-going edge in an argument on all the internal vertices in the other argument. For the Schouten bracket of a k-vector with an ℓ-vector, the rule of signs is this. For the sake of definition, enumerate the sinks in the first and second arguments by using $0, \ldots, k-1$ and $0, \ldots, \ell-1$, respectively. Then the arrow into the jth sink in the second argument acts on the internal vertices of the first argument, acquiring the sign factor $(-)^j$; here $0 \leqslant j < \ell$. On the other hand, the arrow to the ith sink in the first argument acts on the second argument's internal vertices with the sign factor $-(-)^{(k-1)-i}$ for $0 \leqslant i \leqslant k-1$.

The rule of signs, as it has been phrased above, is valid — provided that, for a k-vector $\mathcal{X}$ and ℓ-vector $\mathcal{Y}$, the numbers $0, \ldots$ of the k (or $k-1$) sinks originating in the $(k+\ell-1)$-vector $[\![\mathcal{X},\mathcal{Y}]\!]$ from the first argument $\mathcal{X}$ *precede* the numbers of $\ell-1$ (resp., ℓ) sinks originating from $\mathcal{Y}$ in the overall enumeration of those $k+\ell-1$ sinks.[6] For example, it is this ordering of sinks using $1 \prec 2$ which is shown in (6),

$[\![$  $]\!] =$ 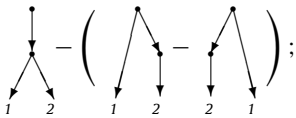 ; (6)

here $k=2$, $\ell=1$ and the enumeration of arguments begins at *1*.

Still let us note that in its realization via Kontsevich graphs, the calculation of the Schouten bracket $[\![\cdot,\cdot]\!]$ effectively amounts to a consecutive plugging of one of its arguments into each of the other argument's sinks (see (6) again). Therefore, it would be more natural to start enumerating the sinks of the graph that acts (on the new content in one of its sinks, possibly the first), but when that new argument is reached, to interrupt and now enumerate the argument's own sinks, then continuing the enumeration of sinks (if there still remain any to be counted) in the graph that acts. This change of enumeration strategy comes at a price of having extra sign factors in front of the graphs. Namely, the arrow into the jth sink in the second argument acquires the extra sign factor $(-)^{j\cdot k}$. Similarly, the arrow to the ith sink in the first argument of $[\![\cdot,\cdot]\!]$ must now be multiplied by $(-)^{\ell\cdot(k-1-i)}$; we recall that $0 \leqslant i \leqslant k$ and $0 \leqslant j < \ell$. We note that for k and ℓ even (e.g., $k=2$ and $\ell=2$ in formula (9)) no extra sign factors appear at all from the re-ordering at a price of $(-)^{j\cdot k}$ and $(-)^{\ell\cdot(k-1-i)}$. For example, such is the final ordering of the $3 = 2+1 = 1+2$ sinks which is shown in Fig. 3.

Summarizing, to be Poisson a bi-vector $\mathcal{P}$ must satisfy the *master-equation*,

$$[\![\mathcal{P},\mathcal{P}]\!] = 0, \tag{7}$$

of which formula (4) is the component expansion with respect to the indices (i,j,k) in the tri-vector $[\![\mathcal{P},\mathcal{P}]\!](\boldsymbol{x},\boldsymbol{\xi})$.

Definition 2. Let $\mathcal{P}$ be a Poisson bi-vector on the manifold N^n at hand and consider its deformation $\mathcal{P} \mapsto \mathcal{P} + \varepsilon\mathcal{Q}(\mathcal{P}) + \bar{o}(\varepsilon)$. We say that after such deformation the bi-vector stays *infinitesimally Poisson* if

$$[\![\mathcal{P}+\varepsilon\mathcal{Q}(\mathcal{P})+\bar{o}(\varepsilon), \mathcal{P}+\varepsilon\mathcal{Q}(\mathcal{P})+\bar{o}(\varepsilon)]\!] = \bar{o}(\varepsilon), \tag{1′}$$

that is, the master-equation is still satisfied up to $\bar{o}(\varepsilon)$ for a given solution $\mathcal{P}$ of (7).

Remark 5. Nowhere above should one expect that the leading deformation term $\mathcal{Q}$ in $\mathcal{P}+\varepsilon\mathcal{Q}+\bar{o}(\varepsilon)$ itself would be a Poisson bi-vector. This may happen for $\mathcal{Q}$ only incidentally.

Expanding the left-hand side of Eq. (1) and using the shifted-graded skew-symmetry of the Schouten bracket $[\![\cdot,\cdot]\!]$, we extract the deformation equation

$$[\![\mathcal{P},\mathcal{Q}]\!] \doteq 0 \qquad \text{via } [\![\mathcal{P},\mathcal{P}]\!] = 0. \tag{2}$$

[5] In the set-up of infinite jet spaces $J^\infty(\pi)$ (see [8] and [5,9,10]) the four partial derivatives in formula (5) for $[\![\cdot,\cdot]\!]$ become the variational derivatives with respect to the same variables, which now parametrize the fibres in the Whitney sum $\pi \times_{M^m} \Pi\widehat{\pi}$ of (super-)bundles over the m-dimensional base M^m.

[6] Such is the default convention which formula (5) suggests for the product of parity-odd variables ξ_{i_α}, where $1 \leqslant \alpha \leqslant k+\ell-1$.

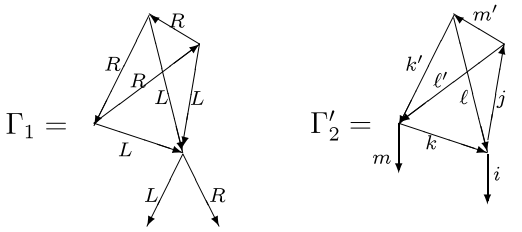

Fig. 2. The Kontsevich tetrahedral graphs encode two bi-linear bi-differential operators on the product $C^\infty(N^n) \times C^\infty(N^n)$.

Let us consider a class of its solutions $\mathcal{Q} = \mathcal{Q}(\mathcal{P})$ which are universal with respect to all finite-dimensional affine Poisson manifolds $(N^n, \mathcal{P})$.

1.2. The Kontsevich tetrahedral flow

In the paper [1], Kontsevich proposed a particular construction of infinitesimal deformations $\mathcal{P} \mapsto \mathcal{P} + \varepsilon\mathcal{Q}(\mathcal{P}) + \bar{o}(\varepsilon)$ for Poisson structures on affine real manifolds. One such flow $\dot{\mathcal{P}} = \mathcal{Q}(\mathcal{P})$ on the space of Poisson bi-vectors $\mathcal{P}$ is associated with the complete graph on four vertices, that is, the tetrahedron. Up to symmetry, there are two essentially different ways, resulting in Γ_1 and Γ_2', to orient its edges, provided that every vertex is a source for two arrows and, as an elementary count suggests, there are two arrows leaving the tetrahedron and acting on the arguments of the bi-differential operator which the tetrahedral graph encodes. The two oriented tetrahedral graphs are shown in Fig. 2. Unlike the operator encoded by Γ_1, that of Γ_2' is generally speaking not skew-symmetric with respect to its arguments. By definition, put $\Gamma_2 := \frac{1}{2}(\Gamma_2'(1,2) - \Gamma_2'(2,1))$ to extract the antisymmetric part, that is, the bi-vector encoded by Γ_2'. Explicitly, the quartic-nonlinear differential polynomials $\Gamma_1(\mathcal{P})$ and $\Gamma_2(\mathcal{P})$, depending on a Poisson bi-vector $\mathcal{P}$, are given by the formulae

$$\Gamma_1(\mathcal{P}) = \sum_{i,j=1}^{n} \left(\sum_{k,\ell,m,k',\ell',m'=1}^{n} \frac{\partial^3 \mathcal{P}^{ij}}{\partial x^k \partial x^\ell \partial x^m} \frac{\partial \mathcal{P}^{kk'}}{\partial x^{\ell'}} \frac{\partial \mathcal{P}^{\ell\ell'}}{\partial x^{m'}} \frac{\partial \mathcal{P}^{mm'}}{\partial x^{k'}} \right) \frac{\partial}{\partial x^i} \wedge \frac{\partial}{\partial x^j} \tag{8a}$$

and

$$\Gamma_2(\mathcal{P}) = \sum_{i,m=1}^{n} \left(\sum_{j,k,\ell,k',\ell',m'=1}^{n} \frac{\partial^2 \mathcal{P}^{ij}}{\partial x^k \partial x^\ell} \frac{\partial^2 \mathcal{P}^{km}}{\partial x^{k'} \partial x^{\ell'}} \frac{\partial \mathcal{P}^{k'\ell}}{\partial x^{m'}} \frac{\partial \mathcal{P}^{m'\ell'}}{\partial x^j} \right) \frac{\partial}{\partial x^i} \wedge \frac{\partial}{\partial x^m}, \tag{8b}$$

respectively. To construct a class of flows on the space of bi-vectors, Kontsevich suggested to consider linear combinations, balanced by using the ratio $a : b$, of the bi-vectors Γ_1 and Γ_2. We recall from Section 1.1 that every internal vertex of each graph is inhabited by a copy of a given Poisson bi-vector $\mathcal{P}$, so that the linear combination of two graphs encodes the bi-vector $\mathcal{Q}_{a:b}(\mathcal{P}) = a \cdot \Gamma_1(\mathcal{P}) + b \cdot \Gamma_2(\mathcal{P})$, quartic in $\mathcal{P}$ and balanced using $a : b$. We now inspect at which ratio $a : b$ the bi-vector $\mathcal{P} + \varepsilon\mathcal{Q}_{a:b}(\mathcal{P}) + \bar{o}(\varepsilon)$ stays infinitesimally Poisson, that is,

$$[\![\mathcal{P} + \varepsilon\mathcal{Q}_{a:b}(\mathcal{P}) + \bar{o}(\varepsilon), \mathcal{P} + \varepsilon\mathcal{Q}_{a:b}(\mathcal{P}) + \bar{o}(\varepsilon)]\!] = \bar{o}(\varepsilon). \tag{1}$$

The left-hand side of the deformation equation,

$$[\![\mathcal{P}, \mathcal{Q}_{a:b}(\mathcal{P})]\!] \doteq 0 \qquad \text{via } [\![\mathcal{P}, \mathcal{P}]\!] = 0, \tag{2}$$

can be seen in terms of graphs:

$$[\![\mathcal{P}, a \cdot \Gamma_1 + b \cdot \Gamma_2]\!] = \left[\!\!\left[\right.\right. \quad , a \cdot \quad + \frac{b}{2} \cdot \left(\quad - \quad \right) \left.\right]\!\!\right]. \tag{9}$$

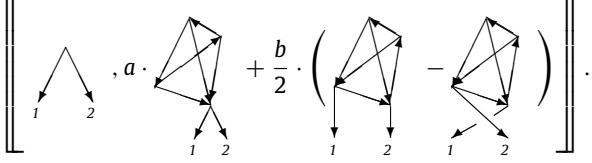

Let $a : b = 1 : 6$ (specifically, $a = \frac{1}{4}$ and $b = \frac{3}{2}$). Then the left-hand side of (2) takes the shape depicted in Fig. 3. After the expansion of Leibniz rules and skew-symmetrization, the sum in Fig. 3 simplifies to 39 graphs; they are listed in Table 2. Collecting, we conclude that the left-hand side of (2) is the sum of 9 manifestly skew-symmetric expressions, see Fig. 4 (and Table 3 in Appendix A). For example, when outlining a proof of our main theorem, we shall explain how the coefficient $-\frac{1}{2}$ of the first and second graphs in Fig. 4 is accumulated from the terms on the right-hand side of (10). Simultaneously, we shall track how the coefficients cancel out for the two other graphs which are produced by expanding the same Leibniz rules (that gave the above two graphs).

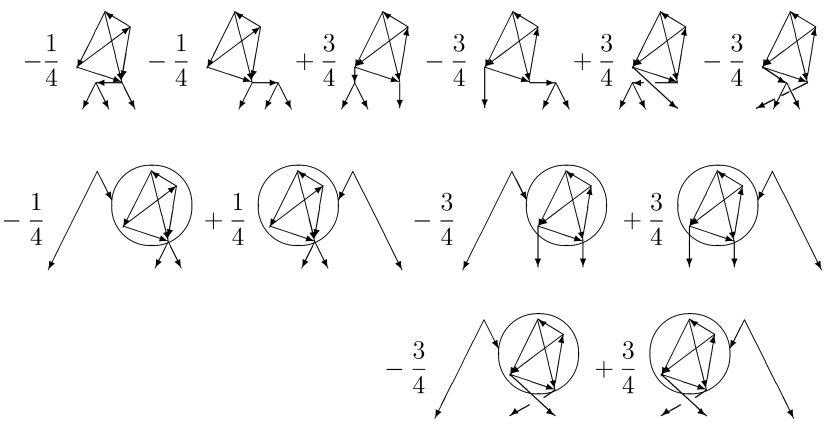

Fig. 3. Incoming arrows act on the content of boxes via the Leibniz rule; to obtain the tri-vector, the entire picture must be skew-symmetrized over the content of three sinks using $\sum_{\sigma\in S_3}(-)^\sigma$. Expanding and skew-symmetrizing, one obtains 39 graphs on the left-hand side of (2).

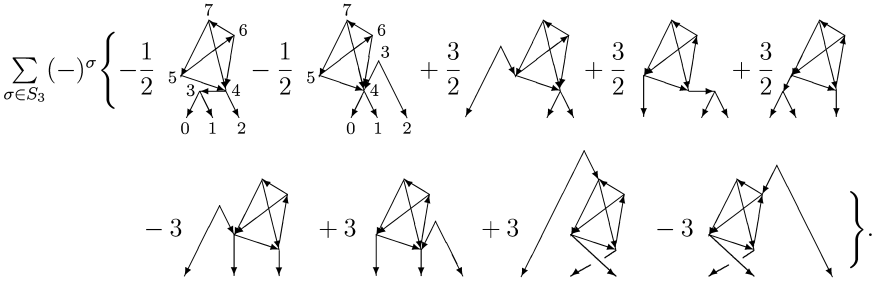

Fig. 4. This sum of graphs is the skew-symmetrized content of Fig. 3. In what follows, we realize these 9 terms on the left-hand side of (2) by using an operator $\lozenge$ acting, on the right-hand side of (10), on the Jacobiator (4).

1.3. Main result

The reason why we are particularly concerned with the ratio $a : b = 1 : 6$ is that this condition is *necessary* for Eq. (2) to hold. This has been proved in [2] by producing examples of Poisson bi-vector $\mathcal{P}$ such that $[\![\mathcal{P}, \mathcal{Q}_{a:b}(\mathcal{P})]\!] = 0$ only when $a : b = 1 : 6$. Let us now inspect whether this condition is also sufficient. The task is to factorize the content of Fig. 4 through the Jacobi identity in (4).

We first examine the mechanism for the tri-vector $[\![\mathcal{P}, \mathcal{Q}_{1:6}(\mathcal{P})]\!]$ in (2) to vanish by virtue of the Jacobi identity $\mathrm{Jac}(\mathcal{P}) = 0$ for a given Poisson bi-vector $\mathcal{P}$ on an affine manifold N^n of any dimension. We claim that the Jacobiator $\mathrm{Jac}_{\mathcal{P}}(\cdot,\cdot,\cdot)$ is not necessarily (indeed, far not always!) evaluated at the three arguments f, g, h of the tri-vector $[\![\mathcal{P}, \mathcal{Q}_{1:6}(\mathcal{P})]\!]$. A sample graph that can actually appear in such factorizing operators $\lozenge$ is drawn in Fig. 5.

Lemma 1 (*[11]*). *A tri-differential operator* $C = \sum_{|I|,|J|,|K|\geqslant 0} c^{IJK}\ \partial_I \otimes \partial_J \otimes \partial_K$ *with coefficients* $c^{IJK} \in C^\infty(N^n)$ *vanishes identically iff all its homogeneous components* $C_{ijk} = \sum_{|I|=i,|J|=j,|K|=k} c^{IJK}\ \partial_I \otimes \partial_J \otimes \partial_K$ *vanish for all differential orders* (i, j, k) *of the respective multi-indices* (I, J, K)*; here* $\partial_L = \partial_1^{\alpha_1} \circ \cdots \circ \partial_n^{\alpha_n}$ *for a multi-index* $L = (\alpha_1, \ldots, \alpha_n)$.

In practice, Lemma 1 states that for every arrow falling on the Jacobiator $\mathrm{Jac}_{\mathcal{P}}(1, 2, 3)$ – for which, in turn, a triple of arguments *1*, *2*, *3* is specified – the expansion of the Leibniz rule yields four fragments which vanish separately: e.g., we have that

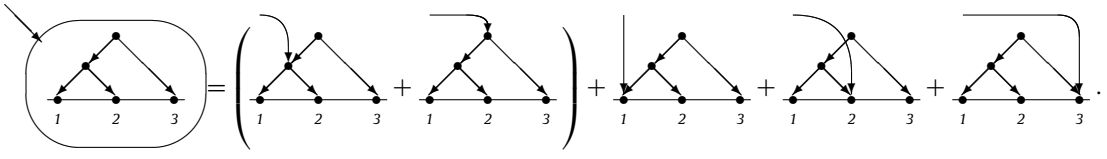

Namely, there is the fragment such that the derivation acts on the content $\mathcal{P}$ of the Jacobiator's two internal vertices, and there are three fragments such that the arrow falls on the first, second, or third argument of the Jacobiator. Now it is readily seen that the action of a derivative ∂_i on an argument of the Jacobiator amounts to an appropriate redefinition of that

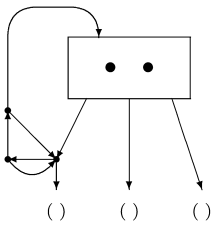

- There is a cycle,
- there is a loop,
- there are no tadpoles in this graph,
- an arrow falls back on $\mathrm{Jac}(\mathcal{P})$,
- and $\mathrm{Jac}(\mathcal{P})$ does not stand on all of the three sinks.

Fig. 5. This is an example of Leibniz graph of which the factorizing operators can consist.

argument: $\partial_i\big(\mathrm{Jac}_{\mathcal{P}}(1,2,3)\big) =$

$$\underbrace{\big(\partial_i \mathrm{Jac}_{\mathcal{P}}\big)(1,2,3)}_{=0} + \underbrace{\mathrm{Jac}_{\mathcal{P}}\big(\partial_i(1),2,3\big)}_{=0} + \underbrace{\mathrm{Jac}_{\mathcal{P}}\big(1,\partial_i(2),3\big)}_{=0} + \underbrace{\mathrm{Jac}_{\mathcal{P}}\big(1,2,\partial_i(3)\big)}_{=0} = 0.$$

Let us introduce a name for the (class of) graphs which make the first term – out of four – in the expansion of Leibniz rule in the above formula.

Definition 3. A *Leibniz graph* is a graph whose vertices are either sinks, or the sources for two arrows, or the Jacobiator (which is a source for three arrows). There must be at least one Jacobiator vertex. The three arrows originating from a Jacobiator vertex must land on three distinct vertices. Each edge falling on a Jacobiator works by the Leibniz rule on the two internal vertices in it.

An example of a Leibniz graph is given in Fig. 5. Every Leibniz graph can be expanded to a sum of Kontsevich graphs, by expanding both the Leibniz rule(s) and all copies of the Jacobiator; e.g. see (12). In this way Leibniz graphs also encode (poly)differential operators, depending on the bi-vector $\mathcal{P}$ and the tri-vector $\mathrm{Jac}(\mathcal{P})$.

Proposition 2. *For every Poisson bi-vector $\mathcal{P}$ the value – at the Jacobiator* $\mathrm{Jac}(\mathcal{P})$ *– of every (poly)differential operator encoded by the Leibniz graph(s) is zero.*

Theorem 3. *There exists a polydifferential operator*

$$\Diamond \in \mathit{PolyDiff}\left(\Gamma\left(\bigwedge\nolimits^2 TN^n\right) \times \Gamma\left(\bigwedge\nolimits^3 TN^n\right) \to \Gamma\left(\bigwedge\nolimits^3 TN^n\right)\right)$$

which solves the factorization problem

$$[\![\mathcal{P}, \mathcal{Q}_{1:6}(\mathcal{P})]\!](f,g,h) = \Diamond\big(\mathcal{P}, \mathrm{Jac}_{\mathcal{P}}(\cdot,\cdot,\cdot)\big)(f,g,h). \tag{10}$$

The polydifferential operator $\Diamond$ is realized using Leibniz graphs in formula (11) *.*

Corollary 4 (*Main Result*)**.** *Whenever a bi-vector $\mathcal{P}$ on an affine real manifold N^n is Poisson, the deformation $\mathcal{P} + \varepsilon\mathcal{Q}_{1:6}(\mathcal{P}) + \bar{o}(\varepsilon)$ using the Kontsevich tetrahedral flow is infinitesimally Poisson.*

Remark 6. It is readily seen that the Kontsevich tetrahedral flow $\dot{\mathcal{P}} = \mathcal{Q}_{1:6}(\mathcal{P})$ is well defined on the space of Poisson bi-vectors on a given affine manifold N^n. Indeed, it does not depend on a choice of coordinates up to their arbitrary affine reparametrizations. In other words, the velocity $\dot{\mathcal{P}}\big|_{\boldsymbol{u}\in N^n}$ does not depend on the choice of a chart $\mathcal{U} \ni \boldsymbol{u}$ from an atlas in which only *affine* changes of variables are allowed. (Let us remember that affine manifolds can of course be topologically nontrivial.)

Suppose however that a given affine structure on the manifold N^n is extended to a larger atlas on it; for the sake of definition let that atlas be a smooth one. Assume that the smooth structure is now reduced – by discarding a number of charts – to another affine structure on the same manifold. The tetrahedral flow $\dot{\mathcal{P}} = \mathcal{Q}_{1:6}(\mathcal{P})$ which one initially had can be contrasted with the tetrahedral flow $\dot{\tilde{\mathcal{P}}} = \mathcal{Q}_{1:6}(\tilde{\mathcal{P}})$ which one finally obtains for the Poisson bi-vector $\tilde{\mathcal{P}}\big|_{\tilde{\boldsymbol{u}}(\boldsymbol{u})} = \mathcal{P}\big|_{\boldsymbol{u}}$ in the course of a nonlinear change of coordinates on N^n. Indeed, the respective velocities $\dot{\mathcal{P}}$ and $\dot{\tilde{\mathcal{P}}}$ can be different whenever they are expressed by using essentially different parametrizations of a neighbourhood of a point $\boldsymbol{u}$ in N^n. For example, the tetrahedral flow vanishes identically when expressed in the Darboux canonical variables on a chart in a symplectic manifold. But after a nonlinear transformation, the right-hand side $\mathcal{Q}_{1:6}(\tilde{\mathcal{P}})$ can become nonzero at the same points of that Darboux chart.

This shows that an affine structure on the manifold N^n is a necessary part of the input data for construction of the Kontsevich tetrahedral flows $\dot{\mathcal{P}} = \mathcal{Q}_{1:6}(\mathcal{P})$.

2. Solution of the factorization problem

Expanding the Leibniz rules in $[\![\mathcal{P}, \mathcal{Q}_{1:6}(\mathcal{P})]\!]$, we obtain the sum of 39 graphs with 5 internal vertices and 3 sinks (so that from Fig. 3 we produce Table 2). By construction, the Schouten bracket $[\![\mathcal{P}, \mathcal{Q}_{1:6}(\mathcal{P})]\!] \in \Gamma(\bigwedge^3 TN^n)$ is a tri-vector on the underlying manifold N^n, that is, it is a totally antisymmetric tri-linear polyderivation $C^\infty(N^n)\times C^\infty(N^n)\times C^\infty(N^n) \to C^\infty(N^n)$. At the same time, we seek to recognize the tri-vector $[\![\mathcal{P}, \mathcal{Q}_{1:6}(\mathcal{P})]\!]$ as the result of application of a (poly)differential operator $\lozenge$ (see (10) in Theorem 3) to the Jacobiator $\mathrm{Jac}(\mathcal{P})$ (see (4)).

We now explain how the operator $\lozenge$ is found.[7] The ansatz for $\lozenge$ is the sum – with undetermined coefficients – of all (separately vanishing) Leibniz graphs containing one Jacobiator and three wedges, and having differential order (1, 1, 1) with respect to the sinks (see Fig. 6). We thus have 28,202 unknowns introduced (counted with possible repetitions of graphs which they refer to). Expanding all the Leibniz rules and Jacobiators, we obtain a sum of Kontsevich graphs with 5 internal vertices on 3 sinks.

As soon as we take into account the order $L \prec R$ and the antisymmetry of graphs under the reversion of that ordering at an internal vertex, the graphs that encode zero differential operators are eliminated.[8] There remain 7,025 admissible graphs with 5 internal vertices on 3 sinks; the coefficient of every such graph is a linear combination of the undetermined coefficients of the Leibniz graphs. In conclusion, we view (10) as the system of 7,025 linear inhomogeneous equations for the coefficients of Leibniz graphs in the operator $\lozenge$. Solving this linear system is a way towards a proof of our main result (which is expressed in Corollary 4). The process of finding a solution $\lozenge$ itself does not constitute that proof. Therefore, the justification of the claim in Theorem 3 will be performed separately. In the meantime, using software tools, we solve the linear algebraic system at hand. The duplications of graph labellings are conveniently eliminated by our request for the program to find a solution with a minimal number of nonzero components. Totally antisymmetric in tri-vector's arguments, the solution consists of 27 Leibniz graphs, which are assimilated into the sum of 8 manifestly skew-symmetric terms as follows:

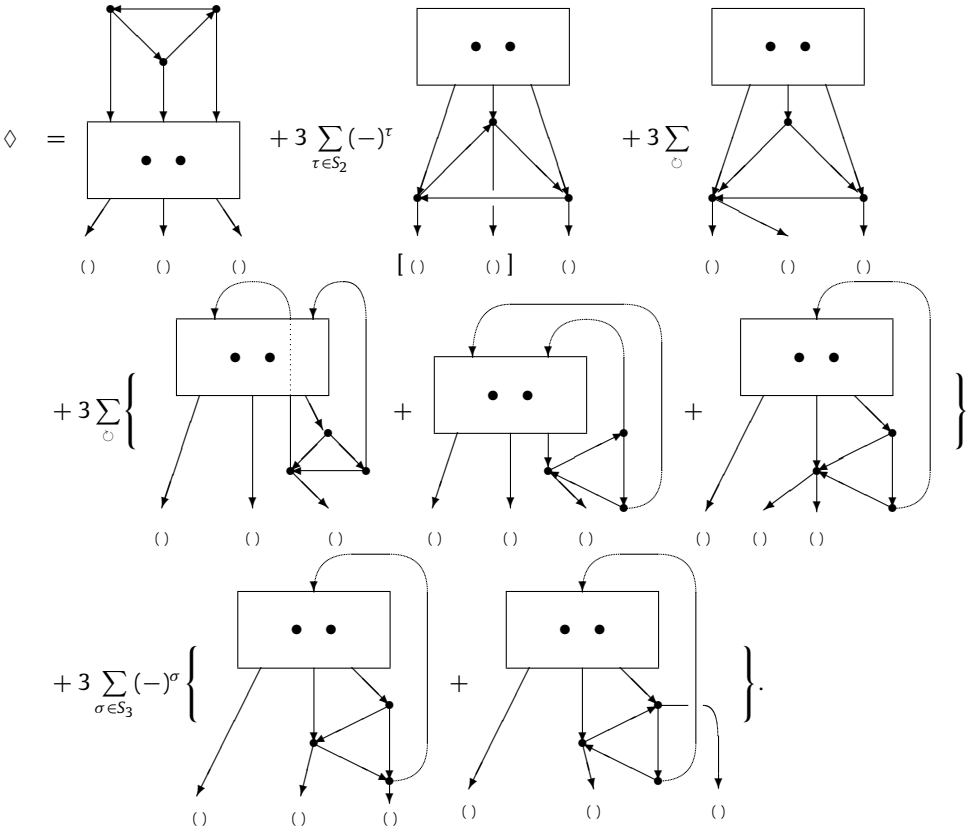

(11)

To display the $L \prec R$ ordering at every internal vertex and to make possible the arithmetic and algebra of graphs, we use the notation which is explained in Appendix A.

[7] Another method for solving the factorization problem is outlined in Appendix B.

[8] The relevant algebra of sums of graphs modulo skew-symmetry and the Jacobi identity has been realized in software by the second author. An implementation of those tools in the problem of high-order expansion of the Kontsevich $\star$-product is explained in a separate paper, see [12].

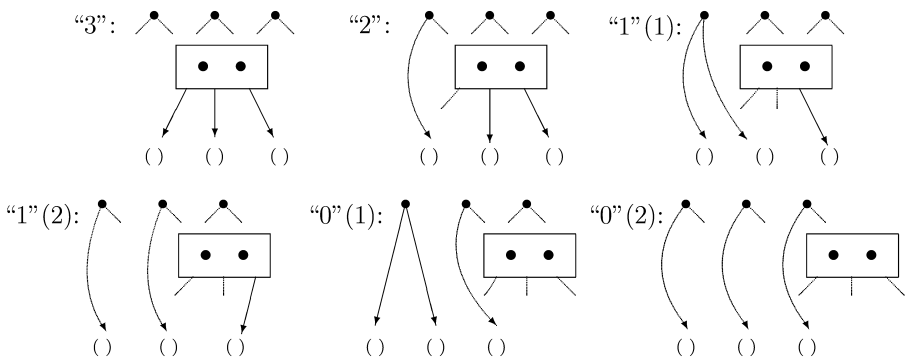

Fig. 6. This is the list of all different types of Leibniz graphs which are linear in the Jacobiator and which have differential order (1, 1, 1) with respect to the sinks. The list is ordered by the number of ground vertices on which the Jacobiator stands.

Remark 7. We remember that the set $\{1, 2, 3\}$ of three arguments of the Jacobiator need not coincide with the set $\{f, g, h\}$ of the arguments of the tri-vector $\Diamond(\mathcal{P}, \mathrm{Jac}(\mathcal{P}))$. Of course, the two sets can intersect; this provides a natural filtration for the components of solution (11). Namely, the number of elements in the intersection runs from three for the first term to zero in the second or third graph.

In fact, Remark 7 reveals a highly nontrivial role of the operator $\Diamond$ in (10). Some of the three internal vertices of its graphs can be arguments of $\mathrm{Jac}(\mathcal{P})$ whereas some of the other such vertices (if any) can be tails for the arrows falling on $\mathrm{Jac}(\mathcal{P})$. In retrospect, the two subsets of such vertices of $\Diamond$ do not intersect; every vertex in the intersection, if it were nonempty, would produce a two-cycle, but there are no "eyes" in (11).

Proof of Theorem 3. So far, we have constructed operator (11); it involves a reasonably small number of Leibniz graphs so that the factorization in (10) can be verified by a straightforward calculation. The sums in (11) contain 27 Leibniz graphs. Now expand all the Leibniz rules; this yields the sum of 201 Kontsevich graphs with 3 sinks and 5 internal vertices: together with their coefficients, they are listed in Table 5 in Appendix A. We claim that by collecting similar terms, one obtains the 39 graphs from the left-hand side of (10), see Fig. 4 and the encoding of those graphs in Table 3. Because we are free to enumerate the five internal vertices in every graph in a way we like, and because the ordering of every pair of outgoing edges is also under our control, at once do we bring all the graphs to their normal form.[9]

It is readily seen that there are many repetitions in Table 5. We must inspect what vanishes and what stays. Let us do a sample reasoning first. Namely, let us inspect the contribution to the left-hand side of (10) from the first term of (11). We have that

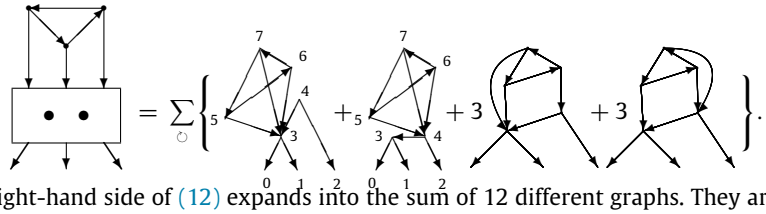

(12)

The right-hand side of (12) expands into the sum of 12 different graphs. They are marked in the first twenty-four lines of Table 5 by $\diamondsuit_i$, $\heartsuit_i$, $\clubsuit_i$ and $\spadesuit_i$ for $1 \leqslant i \leqslant 3$, respectively; by definition, a suit with different values of its subscript i denotes the ith cyclic permutation of the ground vertices for the same graph.[10] For example, the symbols $\diamondsuit_1$, $\diamondsuit_2$, $\diamondsuit_3$ mark the three cyclic permutations of arguments in the first term on the right-hand side of (12). The sum of the first two terms on the right-hand side of (12) – marked by $\diamondsuit_i$ and $\heartsuit_i$, respectively – equals the sum of the first two terms in Fig. 4.[11] At the same time, the sum of the last two terms – whose encodings with coefficients ± 1 are marked by $\clubsuit_i$ and $\spadesuit_i$, respectively – cancels

[9] The normal form of a graph is obtained by running over the group $S_5 \times (\mathbb{Z}_2)^5$ of all the relabellings of internal vertices and swaps $L \rightleftarrows R$ of orderings at each vertex. (We recall that every swap negates the coefficient of a graph; the permutations from S_5 are responsible for encoding a given topological profile in seemingly "different" ways.) By definition, the *normal form* of a graph is the minimal sequence of five ordered pairs of target vertices viewed as 10-digit base-$(3+5)$ numbers. (By convention, the three ordered sinks are enumerated 0, 1, 2 and the internal vertices are the octonary digits $3, \ldots, 7$.)

[10] By taking a graph, placing it consecutively over three cyclic permutations of its sinks' content, *and* bringing the three graph encodings to their normal form, see above, one can obtain an extra sign factor in front of some of these graphs. This is due to a convention about "minimal" graph encoding, not signalling any mismatch in the arithmetic. For example, after the normalization such is the case with the columns in Table 1: each column refers to a cyclic permutation of three arguments and the coefficients in every line would coincide if one encoded the graphs for the last column not using the respective minimal 10-digit octonary numbers. To make all the three coefficients in each line coinciding, it is enough to swap $L \rightleftarrows R$ in one internal vertex in every graph from the third column.

[11] We inspect further that no other graphs in Table 5 make any contribution to the coefficients of these two graphs.

Table 1
The coefficients of graphs marked by the four suits.

$\diamondsuit_1$:	-1	$\diamondsuit_2$:	-1	$\diamondsuit_3$:	$+1$
$\heartsuit_1$:	-1	$\heartsuit_2$:	-1	$\heartsuit_3$:	$+1$
$\clubsuit_1$:	$-1-1-1+3=0$	$\clubsuit_2$:	$-1-1-1+3=0$	$\clubsuit_3$:	$+1+1+1-3=0$
$\spadesuit_1$:	$-1-1-1+3=0$	$\spadesuit_2$:	$-1-1-1+3=0$	$\spadesuit_3$:	$+1+1+1-3=0$

against the contributions from the fourth and sixth terms in solution (11) — with coefficients ± 3, also marked by $\clubsuit_i$ and $\spadesuit_i$ in the rest of Table 5. In Table 1 we calculate the coefficient of each graph marked by the respective indexed symbol.

Now, in the same way all other similar terms are collected. There remain only 39 terms with nonzero coefficients. One verifies that those 39 terms are none other than the entries of Table 2, that is, realizations of the 39 graphs on the left-hand side of (10). This shows that Eq. (10) holds for the operator $\lozenge$ contained in (11). □

Remark 8. Operator (11) is not a unique solution of factorization problem (10). We claim that apart from this sum of 27 Leibniz graphs, there is another solution which consists of 112 Leibniz graphs; it is also linear with respect to the Jacobiator (that is, its realization in the form $\lozenge(\mathcal{P}, \mathrm{Jac}(\mathcal{P}), \mathrm{Jac}(\mathcal{P}))$ is not possible).

Discussion

Non-triviality

A flow specified on the space of Poisson bi-vectors by using the Kontsevich graphs can be Poisson cohomology trivial modulo a sum of Leibniz graphs that would vanish identically at any Poisson structure. However, this is not the case of the Kontsevich tetrahedral flow $\dot{\mathcal{P}} = \mathcal{Q}_{1:6}(\mathcal{P})$.

Proposition 5. *There is no* 1*-vector field* $\mathfrak{X}$ *encoded over* N^n *by the Kontsevich graphs and there is no operator* ∇ *encoded using the Leibniz graphs such that*

$$\mathcal{Q}_{1:6}(\mathcal{P}) = [\![\mathcal{P}, \mathfrak{X}]\!] + \nabla(\mathcal{P}, \mathrm{Jac}(\mathcal{P})).$$

The claim is established by a run-through over all Kontsevich graphs with three internal vertices and one sink (making an ansatz for $\mathfrak{X}$) and all Leibniz graphs (in the operator ∇) with two copies of $\mathcal{P}$ and one Jacobiator in the internal vertices; all such graphs of both types are taken with undetermined coefficients. The resulting inhomogeneous linear algebraic system has no solution.

Integrability

By using the technique of Kontsevich graphs one can proceed with a higher order expansion of the tetrahedral deformation,

$$\mathcal{P} \mapsto \mathcal{P} + \varepsilon\mathcal{Q}_{1:6}(\mathcal{P}) + \varepsilon\mathcal{R}(\mathcal{P}) + \cdots + \bar{o}(\varepsilon^d), \quad d \geqslant 2,$$

for Poisson structures $\mathcal{P}$. Assuming that the master-equation holds up to $\bar{o}(\varepsilon^d)$,

$$[\![\mathcal{P} + \varepsilon\mathcal{Q}_{1:6}(\mathcal{P}) + \varepsilon\mathcal{R}(\mathcal{P}) + \cdots + \bar{o}(\varepsilon^d), \mathcal{P} + \varepsilon\mathcal{Q}_{1:6}(\mathcal{P}) + \varepsilon\mathcal{R}(\mathcal{P}) + \cdots + \bar{o}(\varepsilon^d)]\!] \doteq \bar{o}(\varepsilon^d) \quad \text{via } [\![\mathcal{P}, \mathcal{P}]\!] = 0, \tag{13}$$

we obtain a chain of linear equations for the higher order expansion terms, namely,

$$2[\![\mathcal{P}, \mathcal{R}(\mathcal{P})]\!] + [\![\mathcal{Q}_{1:6}(\mathcal{P}), \mathcal{Q}_{1:6}(\mathcal{P})]\!] \doteq 0 \qquad \text{via } [\![\mathcal{P}, \mathcal{P}]\!] = 0, \text{ etc.} \tag{14}$$

A solution consisting of $\mathcal{R}(\mathcal{P})$ and consecutive terms at higher powers of the deformation parameter[12] can be sought using the same factorization techniques and computer-assisted proof schemes [12] which have been implemented in this paper — whenever such solution actually exists. It is clear that there can be Poisson cohomological obstructions to resolvability of cocycle conditions (14). Hence the integrability issue for the Kontsevich tetrahedral flow may be Poisson model-dependent, unlike the universal nature of such deformation's infinitesimal part.

[12] In every graph at ε^k the number of internal vertices is $3k + 1$.

Table 2
Machine-readable encoding of Fig. 3.

1.1	3	5	4 2 0 1 4 6 4 7 4 5	1/4	7.1	3	5	6 2 7 0 1 4 4 5 5 6	3/4
1.2	3	5	4 0 1 2 4 6 4 7 4 5	1/4	7.2	3	5	6 0 7 1 2 4 4 5 5 6	3/4
1.3	3	5	4 1 2 0 4 6 4 7 4 5	1/4	7.3	3	5	6 1 7 2 0 4 4 5 5 6	3/4
2.1	3	5	7 0 3 5 3 6 3 4 1 2	1/4	8.1	3	5	7 2 7 0 1 4 4 5 5 6	3/4
2.2	3	5	7 1 3 5 3 6 3 4 2 0	1/4	8.2	3	5	7 0 7 1 2 4 4 5 5 6	3/4
2.3	3	5	7 2 3 5 3 6 3 4 0 1	1/4	8.3	3	5	7 1 7 2 0 4 4 5 5 6	3/4
3.1	3	5	5 2 0 1 4 6 4 7 4 5	3/4	9.1	3	5	4 2 7 1 0 4 4 5 5 6	−3/4
3.2	3	5	5 0 1 2 4 6 4 7 4 5	3/4	9.2	3	5	4 0 7 2 1 4 4 5 5 6	−3/4
3.3	3	5	5 1 2 0 4 6 4 7 4 5	3/4	9.3	3	5	4 1 7 0 2 4 4 5 5 6	−3/4
4.1	3	5	6 7 0 3 3 4 4 5 1 2	3/4	10.1	3	5	5 2 7 1 0 4 4 5 5 6	−3/4
4.2	3	5	6 7 1 3 3 4 4 5 2 0	3/4	10.2	3	5	5 0 7 2 1 4 4 5 5 6	−3/4
4.3	3	5	6 7 2 3 3 4 4 5 0 1	3/4	10.3	3	5	5 1 7 0 2 4 4 5 5 6	−3/4
5.1	3	5	4 2 7 0 1 4 4 5 5 6	3/4	11.1	3	5	6 2 7 1 0 4 4 5 5 6	−3/4
5.2	3	5	4 0 7 1 2 4 4 5 5 6	3/4	11.2	3	5	6 0 7 2 1 4 4 5 5 6	−3/4
5.3	3	5	4 1 7 2 0 4 4 5 5 6	3/4	11.3	3	5	6 1 7 0 2 4 4 5 5 6	−3/4
6.1	3	5	5 2 7 0 1 4 4 5 5 6	3/4	12.1	3	5	7 2 7 1 0 4 4 5 5 6	−3/4
6.2	3	5	5 0 7 1 2 4 4 5 5 6	3/4	12.2	3	5	7 0 7 2 1 4 4 5 5 6	−3/4
6.3	3	5	5 1 7 2 0 4 4 5 5 6	3/4	12.3	3	5	7 1 7 0 2 4 4 5 5 6	−3/4
					13.1	3	5	6 0 7 3 3 4 4 5 1 2	−3/4
					13.2	3	5	6 1 7 3 3 4 4 5 2 0	−3/4
					13.3	3	5	6 2 7 3 3 4 4 5 0 1	−3/4

Table 3
Machine-readable encoding of Fig. 4.

3	5	0 1 2 3 4 6 4 7 4 5	−1/2
3	5	0 4 1 2 4 6 4 7 4 5	−1/2
3	5	0 4 5 6 1 2 5 7 4 5	3/2
3	5	0 1 2 5 6 7 3 4 4 6	3/2
3	5	0 4 5 6 1 2 3 7 3 4	3/2
3	5	0 4 5 6 1 6 2 7 4 5	−3
3	5	0 4 5 6 1 7 5 7 2 4	3
3	5	0 4 1 5 2 6 4 7 4 5	3
3	5	0 4 2 5 6 7 1 4 4 6	−3

Acknowledgements

A. K. thanks M. Kontsevich for posing the problem; the authors are grateful to P. Vanhaecke and A. G. Sergeev for stimulating discussions. The authors are profoundly grateful to the referee for constructive criticism and advice.

This research was supported in part by JBI RUG project 106552 (Groningen) and by the IHÉS and MPIM (Bonn), to which A. K. is grateful for warm hospitality. A. B. and R. B. thank the organizers of the 8th international workshop GADEIS VIII on Group Analysis of Differential Equations and Integrable Systems (12–16 June 2016, Larnaca, Cyprus) for partial financial support and warm hospitality. A. B. and R. B. are also grateful to the Graduate School of Science (Faculty of Mathematics and Natural Sciences, University of Groningen) for financial support. We thank the Center for Information Technology of the University of Groningen for providing access to the Peregrine high performance computing cluster.

Appendix A. Encoding of the solution

Let Γ be a labelled Kontsevich graph with n internal and m external vertices. We assume the ground vertices of Γ are labelled $[0, \ldots, m-1]$ and the internal vertices are labelled $[m, \ldots, m+n-1]$. We define the *encoding* of Γ to be the *prefix* (n, m), followed by a list of *targets*. The list of targets consists of ordered pairs where the kth pair ($k \geqslant 0$) contains the two targets of the internal vertex number $m + k$.

The expansion of the Schouten bracket $[\![\mathcal{P}, \mathcal{Q}_{a:b}]\!]$ for the ratio $a : b = 1 : 6$ depicted in Fig. 3 simplifies to a sum of 39 graphs with coefficients $\pm\frac{1}{4}, \pm\frac{3}{4}$. The encodings of these graphs, followed by their respective coefficients, are listed in Table 2. The graphs are collected into groups of three, consisting of the skew-symmetrization – by a sum over cyclic permutations – of a single graph. Within the encodings in the groups of three, the lists of targets only differ by a cyclic permutation of the target vertices 0, 1, 2.

Consisting of 8 skew-symmetric terms, the solution (see (11)) is encoded in Table 4: the sought-for values of coefficients are written after the encoding of the respective 27 Leibniz graphs. Here the sums over permutations of the ground vertices

Table 4
Machine-readable encoding of solution (11).

1.1	3	5	4656360162	−1	6.1	3	5	1235360364	3
					6.2	3	5	0235361364	−3
2.1	3	5	0415233465	−3	6.3	3	5	4601342465	−3
2.2	3	5	0425133465	3					
					7.1	3	5	1535260364	−3
3.1	3	5	0412343465	−3	7.2	3	5	1535062364	3
3.2	3	5	0123343465	−3	7.3	3	5	0535261364	3
3.3	3	5	0213343465	3	7.4	3	5	2535160364	3
					7.5	3	5	2535061364	−3
4.1	3	5	4516460263	−3	7.6	3	5	0535162364	−3
4.2	3	5	4506461263	3					
4.3	3	5	5635260164	−3	8.1	3	5	1425360364	−3
					8.2	3	5	1523460364	−3
5.1	3	5	1456360263	3	8.3	3	5	0425361364	3
5.2	3	5	0456361263	−3	8.4	3	5	0523461364	3
5.3	3	5	5623460164	−3	8.5	3	5	4605132465	−3
					8.6	3	5	4615032465	3

are expanded (thus making the 27 Leibniz graphs out of the 8 skew-symmetric groups). In every entry of Table 4, the sum of three graphs in Jacobiator (4) is represented by its first term. For all the in-coming arrows, the vertex 6 is the placeholder for the Jacobiator (again, see (4)); in earnest, the Jacobiator contains the internal vertices 6 and 7. This convention is helpful: for every set of derivations acting on the Jacobiator with internal vertices 6 and 7, only the first term is listed, namely the one where each edge lands on 6.

Example 2. The first entry of Table 4 encodes a graph containing a three-cycle over internal vertices 3, 4, 5. Issued from each of these three, the other edge lands on the vertex 6: the placeholder for the Jacobiator. This entry is the first term in (11).

Example 3. The entry 3.1 is one of three terms produced by the third graph in solution (11); the Jacobiator in this entry is expanded using formula (4), resulting in three terms (by definition). It is easy to see that the first term contains picture (3) from Remark 2 as a subgraph. Hence the polydifferential operator encoded by this graph vanishes due to skew-symmetry. However, the other two terms produced in the entry 3.1 by formula (4) do not vanish by skew-symmetry. Likewise, there is one term vanishing by the same mechanism in the entry 3.2 and in 3.3.

The proof of Theorem 3 amounts to expanding the Leibniz rules on Jacobiators in Table 4 according to the rules above (resulting in Table 5, where the prefix "3 5" of each graph has been omitted for brevity), simplifying by collecting terms, and seeing that one obtains Table 3.

Appendix B. Perturbation method

In Section 2, the run-through method gave all the terms at once in the operator $\lozenge$ that establishes the factorization $[\![\mathcal{P}, \mathcal{Q}_{1:6}]\!] = \lozenge(\mathcal{P}, \mathrm{Jac}(\mathcal{P}))$. At the same time, there is another method to find $\lozenge$; the operator $\lozenge$ is then constructed gradually, term after term in (11), by starting with a zero initial approximation for $\lozenge$. This is the perturbation scheme which we now outline. (In fact, the perturbation method was tried first, revealing the typical graph patterns and their topological complexity.)

The difficulty is that because the condition $[\![\mathcal{P}, \mathcal{Q}_{1:6}]\!] = 0$ and the Jacobi identity $[\![\mathcal{P}, \mathcal{P}]\!] = 0$ are valid, it is impossible to factorize one through the other; both are invisible. So, we first make both expressions visible by perturbing the Poisson bi-vector $\mathcal{P} \mapsto \mathcal{P}_\epsilon = \mathcal{P} + \epsilon\Delta$ in such a way that the tri-vector $[\![\mathcal{P}_\epsilon, \mathcal{Q}_{1:6}(\mathcal{P}_\epsilon)]\!]$ and the Jacobiator $[\![\mathcal{P}_\epsilon, \mathcal{P}_\epsilon]\!]$ stop vanishing identically:

$$[\![\mathcal{P}_\epsilon, \mathcal{Q}_{1:6}(\mathcal{P}_\epsilon)]\!] \neq 0 \quad \text{and} \quad [\![\mathcal{P}_\epsilon, \mathcal{P}_\epsilon]\!] \neq 0.$$

To begin with, put $\lozenge := 0$. Now consider a class of Poisson brackets on $\mathbb{R}^3$ (cf. [13]) by using the pre-factor $f(x, y, z)$ and arbitrary function $g(x, y, z)$ in the formula

$$\{u, v\}_\mathcal{P} = f \cdot \det\left(\frac{\partial(g, u, v)}{\partial(x, y, z)}\right);$$

it is helpful to start with some very degenerate dependencies of f and g of their arguments (see [2] and [14]). The next step is to perturb the coefficients of the Poisson bracket $\{\cdot, \cdot\}_\mathcal{P}$ at hand; in a similar way, one starts with degenerate dependency of the perturbation Δ. The idea is to take perturbations which destroy the validity of Jacobi identity for $\mathcal{P}_\epsilon$ in the linear approximation in the deformation parameter ϵ. It is readily seen that the expansion of (10) in ϵ yields the equality

$$[\![\mathcal{P}_\epsilon, \mathcal{Q}_{1:6}]\!](\epsilon) = (\lozenge + \bar{o}(1))([\![\mathcal{P}_\epsilon, \mathcal{P}_\epsilon]\!]) = 2\epsilon \cdot (\lozenge + \bar{o}(1))([\![\mathcal{P}, \Delta]\!]) + (\lozenge + \bar{o}(1))([\![\mathcal{P}, \mathcal{P}]\!]) + \bar{o}(\epsilon).$$

Table 5
Expansion of Leibniz rules on Jacobiators in Table 4.

$\diamondsuit_1$	0123363735	−1		0425671336	−3		0425363416	−3
$\clubsuit_1$	0123363745	−1		0456133523	3		0425361734	−3
$\clubsuit_1$	0123363745	−1		0456135723	−3		0425361436	3
$\spadesuit_1$	0123364745	−1		0456173523	3		0425363714	3
$\clubsuit_1$	0123363745	−1		0456175723	−3		0456132356	−3
$\spadesuit_1$	0123364745	−1		0412343745	−3		0456235713	−3
$\spadesuit_1$	0123364745	−1	$\clubsuit_2$	0412364745	3		0456233516	−3
$\heartsuit_1$	0123464745	−1		0456125745	3		0456172336	3
$\diamondsuit_2$	0412464745	−1		0456125735	3		0456162335	−3
$\clubsuit_2$	0412364745	−1		0456123535	3		0456233715	3
$\clubsuit_2$	0412364745	−1		0456125735	−3		0425133456	3
$\spadesuit_2$	0412363745	−1		0415263435	3		0425671334	3
$\clubsuit_2$	0412364745	−1		0415264735	−3		0425363415	−3
$\spadesuit_2$	0412363745	−1		0456162745	−3		0425163734	−3
$\spadesuit_2$	0412363745	−1		0456162735	−3		0425163435	3
$\heartsuit_2$	0412363735	−1		0425361436	−3		0425361734	3
$\diamondsuit_3$	0213363735	1		0425671436	3		0415233546	3
$\clubsuit_3$	0213363745	1		0415362436	3		0456173723	3
$\clubsuit_3$	0213363745	1		0415672436	−3		0456233514	−3
$\spadesuit_3$	0213364745	1		0456172546	−3		0415672336	−3
$\clubsuit_3$	0213363745	1		0456172536	−3		0415362346	−3
$\spadesuit_3$	0213364745	1		0425163435	−3		0456172336	−3
$\spadesuit_3$	0213364745	1		0425164735	3		0415233456	−3
$\heartsuit_3$	0213464745	1		0415233745	−3		0415672334	−3
	0125363434	−3		0415263745	−3		0415363425	3
	0125364734	3		0456175724	3		0415263734	3
	0125673434	−3		0456175723	3		0415263435	−3
	0125673446	3		0456162335	3		0415362734	−3
	0415264745	3		0456162735	3		0425133546	−3
	0415264735	3		0425133745	3		0456273713	−3
	0415263745	3		0425163745	3		0456133524	3
	0415263735	3		0456275714	−3		0425671336	3
	0425363413	−3		0456275713	−3		0425361346	3
	0425364713	3		0456132536	3		0456132735	−3
	0425671334	−3		0456172536	3		0123343546	3
	0425671346	3		0456123535	−3	$\clubsuit_1$	0123363745	3
	0123343745	−3		0456123735	−3		0125363735	−3
	0125364734	−3		0456373712	−3		0125363734	−3
$\spadesuit_1$	0123364745	3		0456363712	3		0125363434	3
	0125364745	3		0456233515	−3		0125363734	3
	0415672446	3		0456233715	−3		0415362346	3
	0415672346	3		0456173723	−3		0415364723	3
	0415672436	3		0456173523	−3		0415363426	3
	0415672336	3		0456133525	3		0415362734	3
	0456233513	−3		0456133725	3		0415362436	−3
	0456273513	−3		0456273713	3		0415363724	−3
	0456235713	3		0456273513	3		0456132536	−3
	0456275713	3		0412343546	3		0456133725	−3
	0215363434	3	$\spadesuit_2$	0412363745	3		0456133526	3
	0215364734	−3		0456123735	3		0456132735	3
	0215673434	3		0456123734	3		0456132356	3
	0215673446	−3		0425363414	−3		0456135723	3
	0425164745	−3		0425363714	−3		0123343456	−3
	0425164735	−3		0415263735	−3		0123343745	3
	0425163745	−3		0415263734	−3		0123343546	−3
	0425163735	−3		0415363424	3		0213343456	3
	0415363423	3		0415363724	3		0213343745	−3
	0415364723	−3		0425163735	3		0213343546	3
	0415672334	3		0425163734	3		0412343456	−3
	0415672346	−3		0213343546	−3		0412343745	3
	0213343745	3	$\clubsuit_3$	0213363745	−3		0412343546	−3
$\spadesuit_3$	0213364745	−3		0215363735	3		0415233456	3
	0215364734	3		0215363734	3		0415233745	3
	0215364745	−3		0215363434	−3		0415233546	−3
	0425671446	−3		0215363734	−3		0425133456	−3
	0425671436	−3		0425361346	−3		0425133745	−3
	0425671346	−3		0425364713	−3		0425133546	3

Knowing the left-hand side at first order in ϵ and taking into account that $[\![\mathcal{P},\mathcal{P}]\!] \equiv 0$ for the Poisson bi-vector $\mathcal{P}$ which we perturb by Δ, we reconstruct the operator $\Diamond$ that now acts on the known tri-vector $2[\![\mathcal{P},\Delta]\!]$. In this sense, the Jacobiator $[\![\mathcal{P},\mathcal{P}]\!]$ shows up through the term $[\![\mathcal{P},\Delta]\!]$.

For each pair $(\mathcal{P}, \Delta)$, the above balance at ϵ^1 contains sums over indices that mark the derivatives falling on the Jacobiator. By taking those formulae, we guess the candidates for graphs that form the next, yet unknown, part of the operator $\Diamond$. Specifically, we inspect which differential operator(s), acting on the Jacobi identity, becomes visible and we list the graphs that provide such differential operators via the Leibniz rule(s). For a while we keep every such candidate with an undetermined coefficient. By repeating the iteration, now for a different Poisson bi-vector $\mathcal{P}$ or its new, less degenerate perturbation Δ, we obtain linear constraints for the already introduced undetermined coefficients. Simultaneously, we continue listing the new candidates and introducing new coefficients for them.

Remark 9. By translating formulae into graphs, we convert the dimension-dependent expressions into the dimension-independent operators which are encoded by the graphs. An obvious drawback of the method which is outlined here is that, presumably, some parts of the operator $\Diamond$ could always stay invisible for all Poisson structures over $\mathbb{R}^3$ if they show up only in the higher dimensions. Secondly, the number of variants to consider and in practice, the number of irrelevant terms, each having its own undetermined coefficient, grows exponentially at the initial stage of the reasoning.

By following the loops of iterations of this algorithm, we managed to find two non-zero coefficients and five zero coefficients in solution (11). Namely, we identified the coefficient ± 1 for the tripod, which is the first term in (11), and we also recognized the coefficient ± 3 of the sum of 'elephant' graphs, which is the second to last term in (11).

Remark 10. Because of the known skew-symmetry of the tri-vector $[\![\mathcal{P}, \mathcal{Q}_{1:6}]\!]$ with respect to its arguments f, g, h, finding one term in a sum within formula (11) for $\Diamond$ means that the entire such sum is reconstructed. Indeed, one then takes the sum over a subgroup of S_3 acting on f, g, h, depending on the actual skew-symmetry of the term which has been found.

For instance, the first term in (11), itself making a sum running over $\{\mathrm{id}\} \prec S_3$, is obviously totally antisymmetric with respect to its arguments. The other graph which we found by using the perturbation method (see the last graph in the second line of formula (11)) is skew-symmetric with respect to its second and third arguments but it is not yet totally skew-symmetric with respect to the full set of its arguments. This shows that it suffices to take the sum over the group $\circlearrowleft = A_3 \prec S_3$ of cyclic permutations of f, g, h, thus reconstructing the sixth term in solution (11).

References

[1] M. Kontsevich, Formality conjecture, in: D. Sternheimer, J. Rawnsley, S. Gutt (Eds.), Deformation Theory and Symplectic Geometry, Ascona 1996, in: Math. Phys. Stud., 20, Kluwer Acad. Publ., Dordrecht, 1997, pp. 139–156.
[2] A. Bouisaghouane, A.V. Kiselev, Do the Kontsevich tetrahedral flows preserve or destroy the space of Poisson bi-vectors? J Phys.: Conf. Ser. Proc. XXIV Int. Conf. 'Integrable Systems and Quantum Symmetries' (14–18 June 2016, CVUT Prague, Czech Republic), 2017, 012008, 1–10. Preprint arXiv:1609.06677 [q-alg].
[3] M. Kontsevich, Feynman diagrams and low-dimensional topology, in: First Europ. Congr. of Math., vol. 2, in: Progr. Math., vol. 120, Birkhäuser, Basel, 1994, pp. 97–121.
[4] M. Kontsevich, Homological algebra of mirror symmetry, in: Proc. Internat. Congr. Math. (Zürich, 1994), vol. 1, Birkhäuser, Basel, 1995, pp. 120–139.
[5] A.V. Kiselev, The deformation quantization mapping of Poisson- to associative structures in field theory, 2017. Preprint arXiv:1705.01777 [q-alg], p. 24.
[6] M. Kontsevich, Deformation quantization of Poisson manifolds, Lett. Math. Phys. 66 (3) (2003) 157–216. Preprint q-alg/9709040.
[7] A.V. Kiselev, S. Ringers, A comparison of definitions for the Schouten bracket on jet spaces, in: Proc. 6th Int. Workshop 'Group Analysis of Differential Equations and Integrable Systems' (18–20 June 2012, Protaras, Cyprus), 2013, pp. 127–141. Preprint arXiv:1208.6196 [math.DG].
[8] P.J. Olver, Applications of Lie Groups to Differential Equations, second ed., in: Grad. Texts in Math., vol. 107, Springer–Verlag, NY, 1993.
[9] A.V. Kiselev, The geometry of variations in Batalin–Vilkovisky formalism, J. Phys.: Conf. Ser. 474 (2013) 012024, 1–51. Preprint 1312.1262 [math-ph].
[10] A.V. Kiselev, The calculus of multivectors on noncommutative jet spaces, 2016. Preprint arXiv:1210.0726 (v4) [math.DG], p. 37.
[11] R. Buring, A.V. Kiselev, On the Kontsevich $\star$-product associativity mechanism, PEPAN Lett. 14 (2) (2017) 403–407. Preprint arXiv:1602.09036 [q-alg].
[12] R. Buring, A.V. Kiselev, Software modules and computer-assisted proof schemes in the Kontsevich deformation quantization, 2017. Preprint IHES/M/17/05, p. 50 + xvi.
[13] J. Grabowski, G. Marmo, A.M. Perelomov, Poisson structures: towards a classification, Modern Phys. Lett. A 8 (18) (1993) 1719–1733.
[14] P. Vanhaecke, Integrable systems in the realm of algebraic geometry, in: Lect. Notes Math., vol. 1638, Springer–Verlag, Berlin, 1996.